TRABAJO DE FIN DE GRADO

SHARKS DR1 validation and the quest for Extremely Red Objects

Sergio Saavedra Esquivel

Supervisores: Aurelio Carnero Rosell, Helmut Dannerbauer

UNIVERSIDAD DE LA LAGUNA - FACULTAD DE CIENCIAS

DEPARTAMENTO DE ASTROFÍSICA

Grado en Física

Junio 2021

RESUMEN

En este trabajo se presenta uno de los primeros resultados científicos del proyecto *Southern H-ATLAS Regions K_s-band Survey* (SHARKS), centrado en el estudio de galaxias lejanas en el infrarrojo cercano. Se emplea el primer *Data Release* del proyecto (DR1), que se publicará próximamente, para desarrollar un algoritmo capaz de seleccionar los Objetos Extremadamente Rojos (del inglés, EROs) presentes en el catálogo. Estos objetos se caracterizan por ser brillantes en el infrarrojo cercano, pero muy tenues en el visible. Por lo tanto, se combinan observaciones de SHARKS, en el infrarrojo cercano, con datos en el óptico, en este caso, proporcionados por el *Dark Energy Survey* (DES). Además, dado que la reducción de imágenes del DR1 de SHARKS todavía no se ha hecho pública, se dedica la primera parte de este trabajo a explicar en detalle las distintas comprobaciones llevadas a cabo para validar los datos empleados durante el mismo. En concreto, se analiza la densidad superficial de objetos, la calidad y profundidad de la imagen considerada, y la correcta calibración fotométrica y astrométrica del catálogo. Una vez se verifican todos los aspectos comentados, se da paso a la búsqueda de EROs. Finalmente, se comparan los resultados obtenidos con trabajos previos, para verificar la validez de los mismos.

ABSTRACT

In this work, one of the first scientific results from the Southern H-ATLAS Regions K_s-band Survey (SHARKS) project is presented, focused on the study of distant galaxies in the near-infrared (NIR). The first Data Release of the project (DR1), which will be published very soon, is used to develop an algorithm to select Extremely Red Objects (EROs) present in the catalogue. These are defined as galaxies bright in the NIR, but very faint in the visible. To do this, SHARKS observations are combined with optical data, in this case, provided by the Dark Energy Survey (DES). In addition, as this is the first scientific analysis done on SHARKS, the first part of this work is dedicated to validate the quality of SHARKS DR1. In particular, surface density of objects, image quality and depth, and the photometric and astrometric calibration of the survey are tested. Once data is verified, the quest for EROs begins. Finally, the results obtained are compared with previous works, to verify their validity.

Contents

Chapter 1

Introduction

En este primer capítulo, se recogen las ideas en torno a las que girará todo el trabajo. Primero, introducimos la importancia de estudiar el universo en el infrarrojo cercano. Después, se presenta el concepto de Objetos Extremadamente Rojos (EROs, del inglés Extremely Red Object), que será empleado con frecuencia durante el proyecto, y se comentan los motivos que hacen a estos objetos un interesante campo de estudio en astronomía. Por último, se contextualiza el proyecto SHARKS, con el fin de que el lector conozca los objetivos que motivaron su diseño, y las características del mismo.

The study of the EROs (dust obscured and old galaxies at high redshift) has important astrophysical and cosmological implications, but they are still not very well studied and several questions are still to be solved. In order to answer them, first it is necessary to select large samples of these objects, and, to do this, we need surveys in the near-infrared for their investigation, like the one used in this TFG, the SHARKS project.

1.1 The Universe in the near-infrared

The near-infrared (NIR) is the shorter region of wavelengths in the infrared spectrum, located between the visible and the medium-infrared, from 750 to 2500 nanometres (see Figure 1.1). The study of the sky in the NIR allows us to study objects with an equivalent temperature between 740 and 4000 Kelvin, but most importantly, it allows us to observe objects that are obscured in the visible by dust.

In the NIR, dust is transparent, so by the use of bands in this region of the electromagnetic spectrum is possible to study objects that has been obscured by dust. Likewise, at these wavelengths, high-redshift galaxies are still bright, something that allows us to study these distant objects in more detail.

But the astronomy developed in the NIR is not at all an easy task. At these wavelengths, the thermal radiation from the telescope and the atmosphere affects the measurements, being sometimes larger than the infrared signal from the sources observed. Therefore, the use of special hardware and image reduction techniques is essential to bypass these difficulties in NIR astronomy.

Also, the atmosphere is opaque to certain wavelengths of the NIR, so radiation from outer space only pass through certain wavelength "windows". The bands used in the NIR study (z, Y, K...) should therefore be centered at these atmospheric windows (see Figure 1.2).

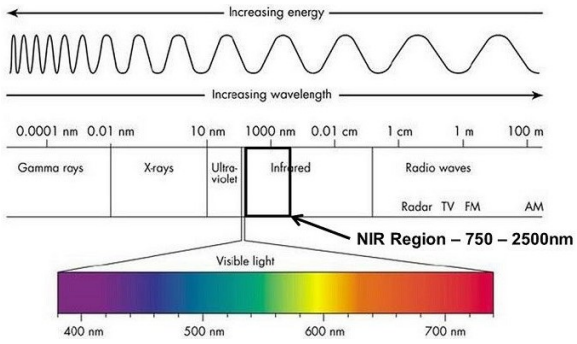

Figure 1.1: *The electromagnetic spectrum. The near-infrared region is defined between 750 and 2500 nanometres, just after the optical region.*[1]

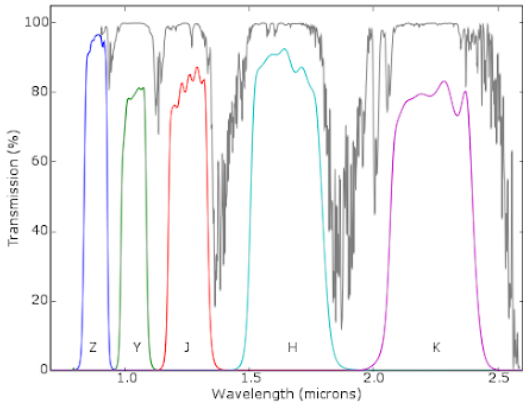

Figure 1.2: *NIR windows (grey), and how the different NIR filters observe through them in the z, Y, J, H and K filters.*[2]

1.2 Extremely Red Objects

Extremely Red Objects (EROs) is a group of extragalactic objects that are very faint in the optical but relatively bright in the NIR *(Daddi et al. 2000)*, which translates in a large magnitude difference between the optical and the near-infrared bands (see Figure 1.3).

They are a difficult to study group of objects, composed mainly by dusty active galaxies, like starbursts or AGNs (Active Galactic nucleus), and ellipticals at moderate to high redshift ($z > 1$). Dust-reddened star-forming galaxies are bright in the NIR because cosmic dust is transparent at these wavelengths, and the old, high redshift galaxies are brighter in these ranges due to the redshift of the spectrum *(Daddi et al. 2000)*.

[1] Process Sensors. Near Infrared Measurements – How Do They Work? `https://www.processsensors.com/whats-new/blog/near-infrared-measurements-how-do-they-work`

[2] Cambridge Astronomy Survey Unit (CASU). WFCAM Filter Set. `http://casu.ast.cam.ac.uk/surveys-projects/wfcam/technical/filter-set`

There are still many questions to be solved about EROs:[3]

1. What is the relative fraction of starbursts and AGN among the ERO population?
2. What are the low redshift descendants of these high-z objects?
3. Is this population a significant component of the Universe at high redshift?
4. What is the contribution of these objects to the total mass density and star-formation rate density of the Universe at $z \approx 1$?
5. EROs are fundamental to understand star formation during the cosmic noon (the star formation peak of the Universe, at $z \approx 2$, when the Universe had ≈ 3.3 Gyrs).

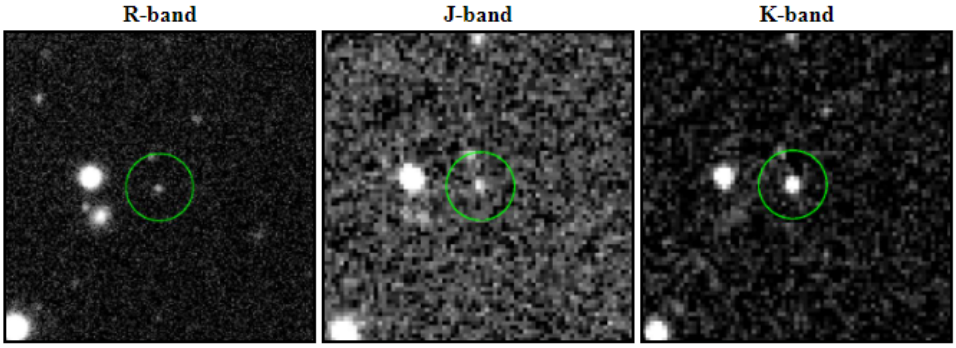

Figure 1.3: *Comparison between optical (R-band) and near-infrared (J and K-bands) images of the faint radio source PDFJ011423 discovered during the Phoenix Deep Survey (Afonso et al. 2001), a typical example of an ERO.*

It is important to notice that ultra-cool dwarfs (UCDs, consisting of low-mass stars and brown dwarfs) also have very red colours, but are not considered EROs. Therefore, they are a potential source of contamination when looking for EROs *(Thompson et al. 1999)*, *(Cuby et al. 1999)*.

1.3 The SHARKS project

The Southern H-ATLAS Regions K_s-Band Survey (SHARKS) is an ESO (European Southern Observatory) public survey focused in the study of distant galaxies in the near-infrared.

As its own name says, it observes the southern galactic region of the sky, by the VISTA telescope in the Paranal observatory, at Chile (Sutherland et al. 2015). The

[3] A. Georgakakis. Research: Extremely Red Objects. `http://members.noa.gr/age/eros.html`

survey will be completed after 1200 hours of exposition with the VIRCAM camera, the NIR camera installed at the telescope.[4]

It is a survey developed over some of the H-ATLAS Regions, the largest extragalactic survey from the *Herschel* telescope *(Eales et al. 2010)*, from which SHARKS observe ≈ 300 square degrees (see Figure 1.4). From the 300 deg^2, around 250 have already been reduced, and the 50 remaining will be observed during 2021 and 2022. SHARKS observations are made using a single near-infrared band, the K_S band, centered at 2.2 *microns*, expecting a magnitude limit of 22.7 mag $[AB, 5\sigma]$.

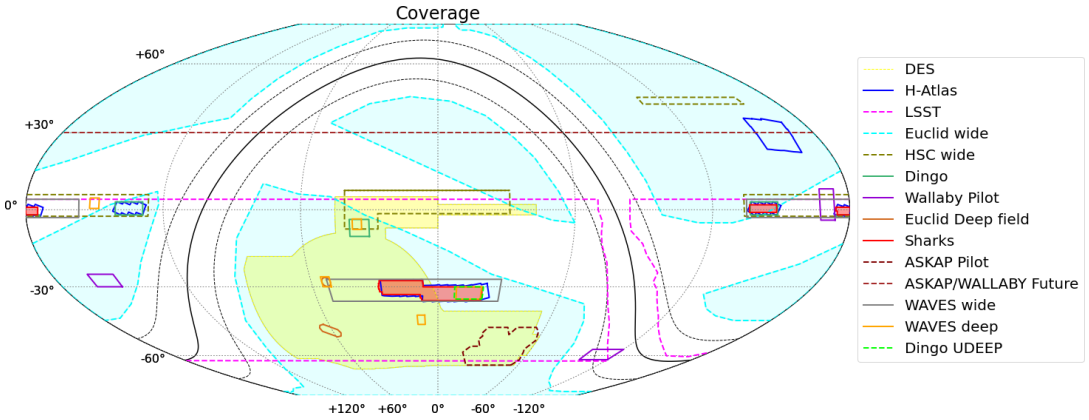

Figure 1.4: *SHARKS footprint (in red) over present and future surveys. It can be seen the overlap with the southern H-ATLAS regions, namely at the GAMA15, GAMA12 and SGP fields.*[5]

The SHARKS project was designed to fill the gap between surveys that cover wide-sky areas and those that cover smaller areas, but have a higher magnitude limit (see Figure 1.5 and Table 1.7). This makes SHARKS ideal to study the formation of galaxies, the origin of galaxies clusters and also to search for cosmological gravitational lenses.

This higher magnitude limit, compared to other previous NIR surveys, like VIKING, translates into the detection of more objects at higher redshifts associated with sources in the H-ATLAS survey, reaching a high completeness up to redshift ≈ 2 (see Figure 1.6).[6]

[4] ESO. VISTA: Visible and Infrared Survey Telescope for Astronomy. `https://vista.maths.qmul.ac.uk`

[5] IAC. SHARKS project website. `http://research.iac.es/proyecto/sharks/pages/en/home.php`

[6] IAC. SHARKS: More than 20 million near-infrared sources across cosmic time. `https://www.youtube.com/watch?v=XAheJ_SpusY&t=1027s`

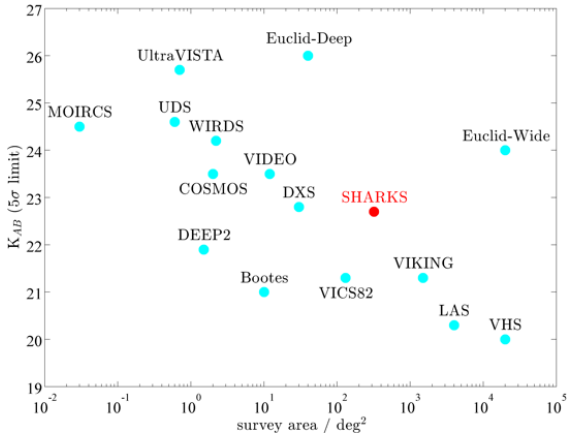

Figure 1.5: *Comparison between area and magnitude limit for surveys in the NIR. SHARKS is highlighted in red (Oteo et al. 2016).*

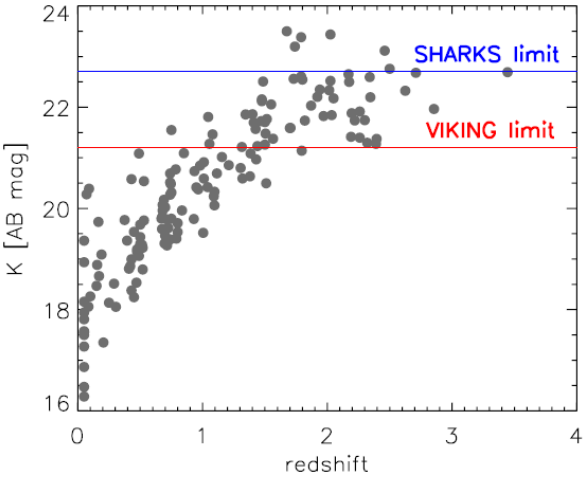

Figure 1.6: *Detection efficiency of H-ATLAS sources by SHARKS and VIKING, as a function of redshift. A magnitude limit of 22.7 is equivalent to observe galaxies up to $z \approx 2$ (Oteo et al. 2017).*

Survey	Depth in K band [AB mag]	Area [deg^2]
UltraVISTA	24.2	~ 1.5
VIDEO	23.5	~ 12
SHARKS	**22.7**	~ 300
VICS82	21.3	~ 130
VIKING	21.2	~ 1500

Table 1.7: *Magnitude limit and area covered by SHARKS and other NIR surveys. It can be seen the position of SHARKS as a wide field area survey, with also a high depth in the K_s band (Oteo et al. 2017).*

Chapter 2

Objectives

El segundo capítulo se centra en mostrar los objetivos que se han planteado durante el desarrollo de este trabajo. El primero de ellos ha sido la validación del catálogo de objetos que compondrá el primer "Data Release" del proyecto SHARKS, y, el segundo, el empleo de estos datos para crear un algoritmo de detección de EROs, que pudiera dar cuenta del potencial que este "survey" tiene para observar y clasificar objetos únicamente brillantes en bandas del infrarrojo cercano. Para llevar a cabo este segundo objetivo, se han empleados también datos del Dark Energy Survey.

After the introduction, the need for surveys that explore the NIR to study unique objects like EROs is clear. In this work, the SHARKS Data Release 1 (DR1) will be firstly validated, and then used to develop an EROs finding algorithm.

2.1 SHARKS DR1 validation

SHARKS DR1 is planned to be released very soon. But first, it is necessary to prove the correctness of the images and the reduction process, by applying a set of different verifications. In particular, we validated DR1 in terms of astrometric and photometric calibration, image quality and depth.

In terms of the astrometric and photometric calibration, we compared SHARKS data with external data from *Gaia* (astrometry), 2MASS (astrometry) and VIKING (photometry), comparing their positions and magnitudes. In terms of image quality, we looked at the angular distribution of different quantities (sky variance, ellipticity and signal to noise), searching for pathological patterns in the data. Finally, depth was estimated for sources with $S/N \simeq 5$ and compared with the expected magnitude limit of $K_s = 22.7\ mag\ [AB, 5\sigma]$. Also, an analysis of DR1 object distribution was made.

After the validation of the data, the DR1 catalogue was used in a scientific study.

2.2 Design and study of an EROs catalogue from SHARKS DR1 in combination with DES

The second objective of this work is the use of SHARKS DR1 to explore the EROs population that are not detectable in the optical, but are bright in the NIR. To do this, an algorithm was developed to select the EROs present in the DR1 catalogue, by the comparison with observations in the optical, in our case, provided by the Dark Energy Survey (DES) *(Abbott et al. 2005)*. The algorithm we present here was developed by the comparison of magnitudes measured in the R-band and in the K_s-band.[3]

But EROs samples suffer from contamination of UCDs. These objects are also bright at red wavelengths due to their low temperature, and they are also difficult to detect in the visible. As we are interested in the study of galaxies, and not stars, the presence of UCDs in the EROs catalogue is undesired, so, in addition to the development of the algorithm to select EROs, we designed another algorithm to filter UCDs from the EROs sample, in order to consider only those objects properly called EROs in the final sample (that means, dusty active galaxies, and elliptical galaxies at $z > 1$). This filtering algorithm was developed taking as reference the star-galaxy classifier used in *Daddi et al. 2000*.

The entire process of the EROs finding can be resumed as:

1. Association between NIR observations and optical ones.
2. Selection of objects by measuring their colours ($R - K_s$).
3. Decontamination from UCDs.

Finally, the results of the EROs finding were compared with those obtained in *Daddi et al. 2000*, which is our reference article in the study of EROs presented here.

Chapter 3

DATA

A lo largo del Trabajo de Fin de Grado, se han empleado numerosos catálogos astronómicos, provenientes de distintos "surveys" científicos. En este capítulo se incluyen todos los catálogos de datos empleados en el desarrollo del proyecto, y se contextualiza el uso de cada uno de ellos en los distintos procesos llevados a cabo.

During this work, different astronomical catalogues were used to assist in our objectives, both to validate SHARKS data, and to select our EROs sample. But, the basis of our work is the SHARKS DR1 catalogue.

3.1 SHARKS DR1

SHARKS DR1 is obtained from observations of approximately 20 square degrees (deg^2) from the 300 deg^2 that make the whole SHARKS catalogue. SHARKS DR1 will be published in the near future.

In this work, only 7.23 deg^2 from DR1 were used, located in the SGP-East field, that overlaps with DES, which was used to select the EROs sample. Henceforth, the catalogue obtained from these 7.23 deg^2 considered will be called SHARKS DR1, but is important to remember that the public DR1 release will contain around 13 deg^2 of more area. The catalogue used (of 7.23 deg^2) contains 623543 objects.

As anticipated on the previous chapter, the information provided by DES was used in the finding of EROs, and this is thanks to the overlap between SHARKS DR1 and DES (see Figure 3.1), that allows the comparison of SHARKS DR1 NIR data with the optical observation by DES.

SHARKS DR1 data will be found at the ESO archive and in `http://research.iac.es/proyecto/sharks/pages/en/data-releases/dr1.php` once the data is public.

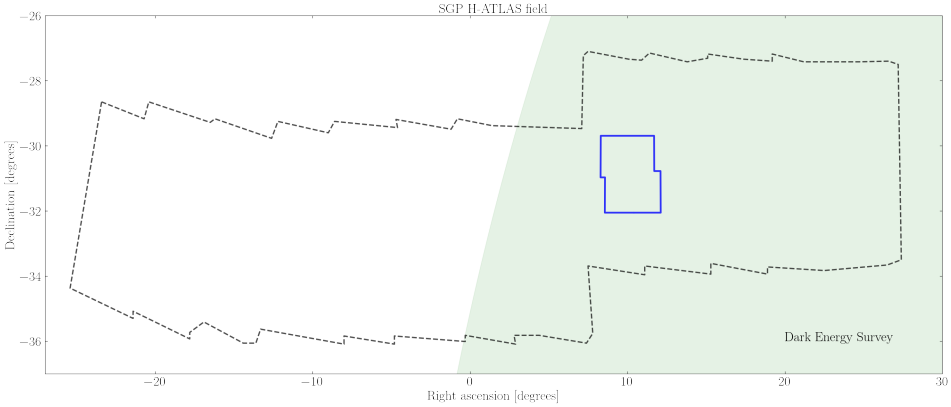

Figure 3.1: *SHARKS DR1 area used in this work (blue) overlapping the area from DES (green) and H-ATLAS (dashed line) (Carnero, priv. comm.).*

3.2 Dark Energy Survey

DES is an optical-NIR survey of 5000 deg^2, focused in the measurement of dark energy and dark matter *(Abbott et al. 2005)*. To do this, the survey use The Dark Energy Camera (DECam) at the Blanco Telescope in Cerro Tololo, Chile. DECam was specially designed to be more sensitive to the red part of the optical spectrum and in the NIR, in comparison to previous instruments *(Honscheid et al. 2008)*. The better sensibility in the red part of the optical and its depth are the reason why this survey was used. The DES catalogue that we used is the one coming from the recent second Data Release of the project *(Abbott et al. 2021)*. This catalogue has benchmark galaxy and stellar samples that contain 543 million and 145 million objects, respectively.

In this work we used the r-band of DES centered at 0.6 microns with the K_s-band from SHARKS (centered at 2.2 microns). The limiting magnitude of r_{DES} is set on $r_{DES} = 25.6\ mag\ [AB, 5\sigma]$.

It is important to recall the difference between the R-band used in [3] and in *Daddi et al. 2000*, and the r-band used by DES. In the cited articles they used the standard R-Johnson filter in Vega calibration, whereas in DES it is the DECam r filter in AB system *(Abbott et al. 2021)*. The difference between magnitudes measured in these bands is given by the next expression (3.1):[7]

$$r_{DES,AB} = R_{AB} + 0.45 = (R_{Vega} + 0.2) + 0.45 \leftrightarrow r_{DES,AB} = R_{Vega} + 0.65 \tag{3.1}$$

In addition with DES, another three catalogues were used during the validation of SHARKS DR1, specifically during the astrometry and photometry verification, two of

[7] M.R. Blanton, et al. Useful Astronomical Data, Ohio State University. `http://www.astronomy.ohio-state.edu/~martini/usefuldata.html`

the most usual tests that are made to astronomical catalogues.

3.3 Catalogues used during the DR1 verification

The use of external data is needed during the validation process of any data-set. The various catalogues that also overlap with SHARKS DR1 and that were used during the verification of it are commented below. To download all these catalogues, we used the Vizier tool, provided by the University of Strasbourg *(Ochsenbein et al. 2000)*.

3.3.1 2MASS

During the astrometrical verification, two widely used catalogues were employed. The first of them was 2MASS (Two Micron All-Sky Survey) *(Skrutskie et al. 2006)*, in particular, it was used the 2MASS All-Sky catalogue of Point Sources *(Cutri et al. 2003)*, with near to 471 million sources detected and a K_s magnitude limit of $K_s = 14.3\ mag\ [Vega, 10\sigma]$

This is an already finished survey that completed its observations in 2001. These were made from two telescopes, one on the northern hemisphere and the other in the southern hemisphere, by the use of three infrared bands, J, H and K_s. The final result was an all-sky map, published in 2003.

This catalogue has been traditionally used to calibrate the astrometry and photometry of subsequent surveys, and it is the catalogue used to calibrate the SHARKS DR1 data.

3.3.2 Gaia

The other catalogue used during the astrometry verification is *Gaia (Prusti et al. 2016)*, in particular the second Data Release of the project *(Brown et al. 2018)*. This second Data Release contains more than 1692 million sources, and has a limiting magnitude of $G = 21\ mag\ [Vega]$.

As a curiosity, although *Gaia* name originally come from "Global Astrometric Interferometer for Astrophysics", the original interferometry technique that was originally planned, changed. Despite the name is still the same, it is no longer an acronym.

This catalogue is built from observations of a space telescope that was launched back in 2013 and is planned to operate until 2022, so it is still an ongoing survey. This ambitious project has many objectives, like measuring the photometry and radial velocity to millions of stars, and, what is more interesting to the astrometrical verification, a mapping of all the Milky Way from the space, evading the distortions that the atmosphere cause to the observations made from earth.

3.3.3 VIKING

The other survey employed was VIKING, that was used in the DR1 photometry verification. Usually, VISTA surveys photometry is calibrated with the use of the 2MASS catalogue *(González-Fernández et al. 2017)*, including SHARKS. But, to validate the SHARKS DR1 photometry, it was decided to use the VIKING catalogue (VISTA Kilodegree Infrared Galaxy Public Survey) *(Edge et al. 2013)*, which is also calibrated with respect to 2MASS.

This is a VISTA NIR survey (similar to SHARKS), that have observed $1350 deg^2$ of sky, in the Z, Y, J, H and K_s bands but to a brighter magnitude limit. As VIKING is a project conducted at the same telescope, and in the same band of observation than SHARKS, it is ideal to make the photometry comparison with SHARKS DR1 catalogue, as this sample is larger than 2MASS.

In this work, we have used the second Data Release of the project, from 2016 *(Edge et al. 2016)*. This Data Release covers $\approx 690 deg^2$ of sky, includes more than 46 million sources and have a K_s band limiting magnitude of $K_s = 21.2\ mag\ [Vega, 5\sigma]$

VIKING is calibrated with respect to Vega, a difference with SHARKS, that is calibrated in the AB system. In theory, since both VIKING and SHARKS are calibrated with respect to 2MASS, this is the only difference we should find when comparing both.

Chapter 4

SHARKS DR1 validation

Tras conocer los distintos catálogos de datos que se usarán durante el TFG, se desarrolla en este cuarto capítulo uno de los dos objetivos principales del trabajo: la validación completa y rigurosa del catálogo que compondrá el primer "Data Release" de SHARKS. Este es un procedimiento extenso que debe ser llevado a cabo realizando una serie de comprobaciones que garanticen la calidad de las observaciones y la correcta reducción de las imágenes obtenidas. Para cada uno de los procesos considerados se detallará la metodología empleada y los resultados que se han obtenido. Finalmente, se considerarán todos los estudios realizados para dar un veredicto sobre la validez o no del catálogo analizado.

To meet the level of precision and confidence required in science, it is essential the use of data that have been previously validated.

To validate SHARKS DR1 catalogue, five different properties of the data were analysed. During the validation, astronomical tools like `DS9` (Appendix A.11) or `Topcat` (Appendix A.12) were used assiduously, together with the development of `Python` programs (Appendix A.2).

The different validation tests applied to SHARKS DR1 data are explained below.

4.1 Object distribution

The first of these steps was the familiarization with the data considered (the 623543 objects detected in the 7.23 deg^2 that will make part of the SHARKS DR1). To start with, we did a visual inspection of the images (using `DS9`), overlaying the catalogue sources on top of the images, to examine if the source extraction was correctly done and to identify regions with possible large portion of spurious detection.

Next, we represented, both in equatorial and galactic coordinates, the density distri-

bution of sources in the footprint, in order to have an idea of how the data distribute over the sky. Equatorial coordinates are the ones that will be used during the whole project. The results obtained are shown in Figure 4.1.

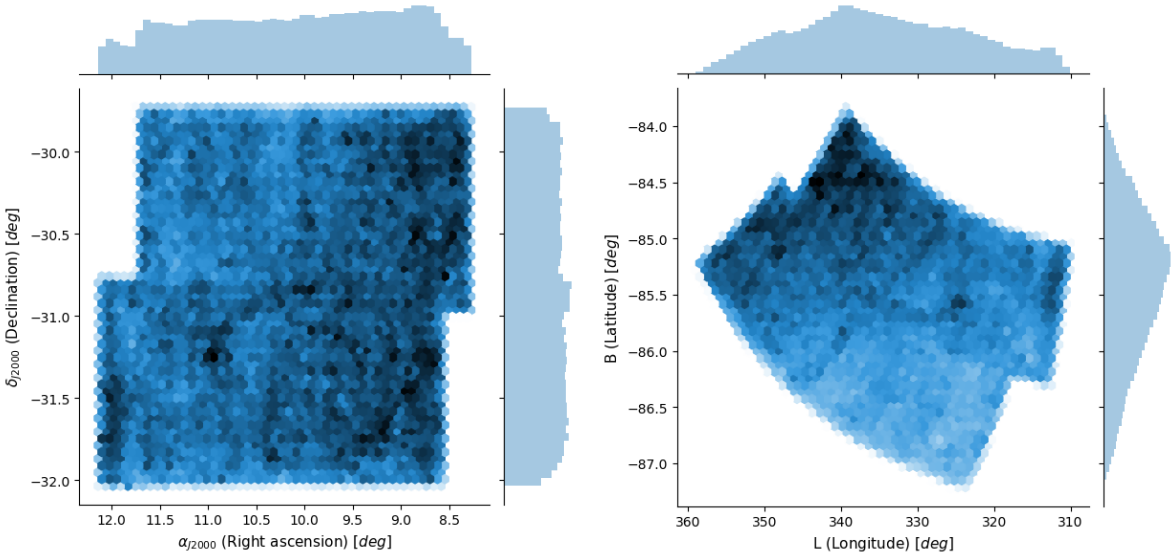

(a) *Equatorial coordinates.* **(b)** *Galactic coordinates.*

Figure 4.1: *Density distribution of the data over the 7.23 deg^2, in equatorial (**(a)**, x-axis = right ascension, y-axis = declination) and galactic coordinates (**(b)**, x-axis = galactic longitude, y-axis = galactic latitude). Darker regions show greater concentration of objects. The side histograms show the variation in the density of sampled objects as a function of each axis.*

The presence of certain zones with overdensities of objects can be observed, especially in the right part of the image (in equatorial coordinates). This is explained by the larger number of exposure time in these regions. The area represented here is obtained from the joining of four coadd images; at the same time, these images are coadded from a mosaic of individual IR detector images. This composition lead to the presence of certain zones with more exposure time than others, that means, areas of higher object density.

In fact, the VIRCAM camera, used in the SHARKS project, has 16 individual detectors. The four coadd images previously commented are made by the overlap of different single-epoch images taken by the VIRCAM camera. To read about the composition of images by the VIRCAM camera, is recommended to consult the next reference: [4]

In addition, it can also be seen the presence of some spots with overdensities, scattered in the footprint, like the one around RA = 11, Dec = -31.4. These spots are caused by diffracted stars, that produce big densities of spurious objects (as it was confirmed with a visual inspection of the images with `DS9`).

In any case, the main objective of this procedure was to observe if any region of

the footprint had miss-samplings, and to ensure the correct detection of objects by the telescope during the observation over all the area considered; and it can be affirmed by this study of the object distribution. The presence of areas with larger exposure time is something completely normal and not worrying, as far as these regions are known.

4.2 Image quality

After analysing the object distribution of the survey, image quality checks were performed, by plotting the change that some variables of interest have over the footprint. By verifying the homogeneity of these variables, the correctness of the data reduction can be ensured. The different variables represented are:

- **Signal to noise ratio (S/N)**: It is an indicative of how significant a detection is over the error: $S/N = \frac{flux}{\sigma(flux)}$. In term of magnitudes, it can be calculated from the error in the magnitude as:[8]

$$\begin{aligned} \sigma(mag) &= -2.5 \times \log_{10}(flux) + 2.5 \times \log_{10}(flux + \sigma(flux)) \\ &= 2.5 \times \log_{10}((flux + \sigma(flux))/flux) \\ &= 2.5 \times log_{10}(1 + N/S) = \mathbf{2.5} \times \mathbf{log_{10}}(\mathbf{1} + \frac{\mathbf{1}}{\mathbf{S/N}}) \end{aligned} \tag{4.1}$$

  By Taylor expansion of this equation, we get to the final expression:

$$\begin{aligned} \sigma(mag) &= 2.5/2.3 \times [N/S - \frac{1}{2}(N/S)^2...] \\ &\approx 1.087 \times (N/S) \end{aligned} \tag{4.2}$$

$$\mathbf{S/N} \approx \frac{\mathbf{1.087}}{\sigma(\mathbf{mag})} \tag{4.3}$$

- **Sky variance**: It is an indicative of the variance of the sky brightness.
- **Ellipticity of galaxies and stars**: It is an indicative of PSF distortions. In the ideal case, the ellipticity of stars should be zero, so a small value for this parameter means a correct image. In the case of galaxies, the mean value should be higher than for stars but, in average, constant across the footprint.

In Figure 4.2 we show the distribution of these variables over the footprint. The colour indicates the value that each source in the catalogue has for each of the variables considered.

[8] M. Bolte. Modern Observational Techniques. `http://www.ucolick.org/~bolte/AY257/s_n.pdf`

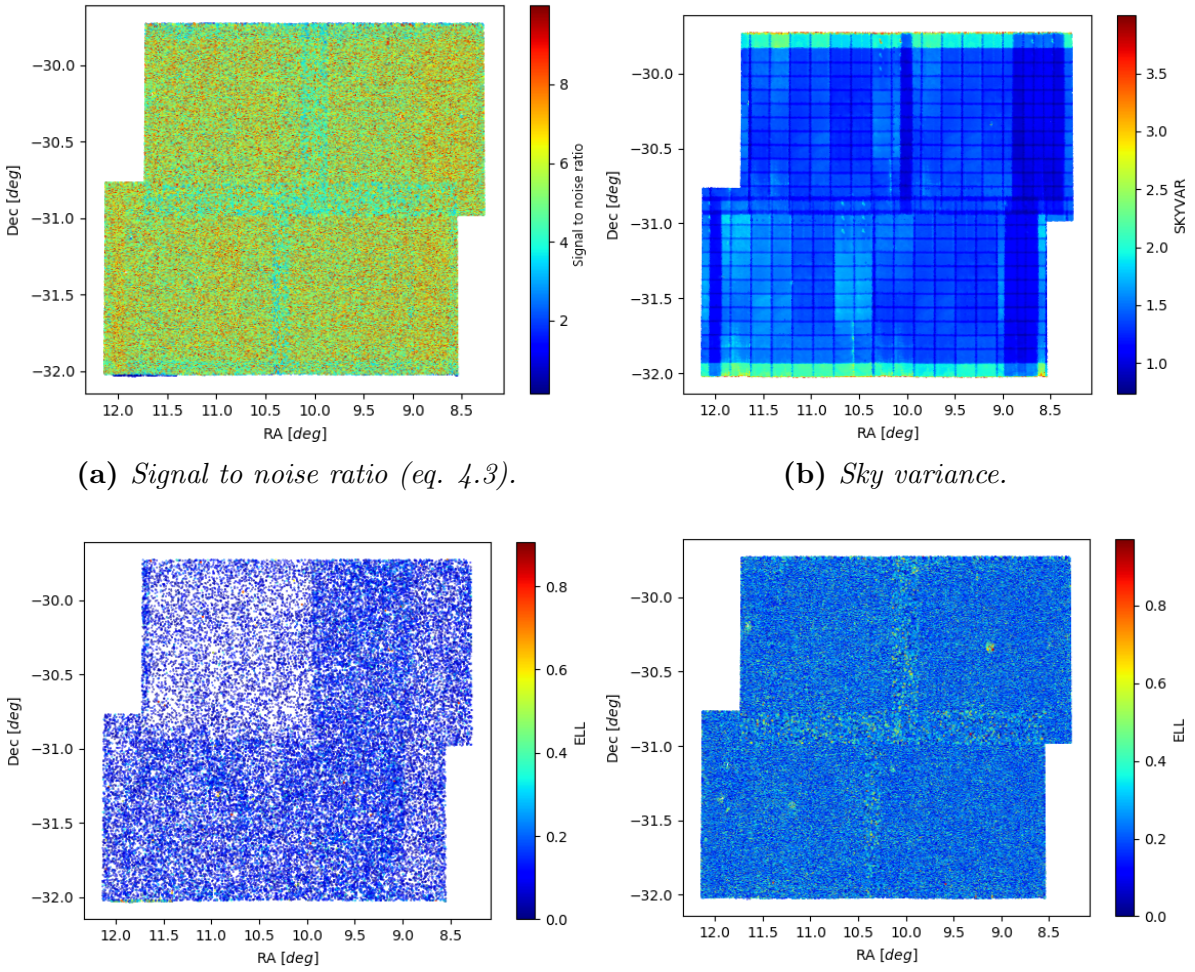

(a) *Signal to noise ratio (eq. 4.3).*

(b) *Sky variance.*

(c) *Star ellipticity.*

(d) *Galaxy ellipticity.*

Figure 4.2: *Angular distribution of variables of interest taken from the sample of objects. The axis shows always the same information, right ascension (RA, horizontal axis) and declination (Dec, vertical axis), both in degrees. The colourbar show the value of the different variables.*

In the sky variance representation (see Figure 4.2b), the detectors distribution commented on the previous section is clearly visible. It can be seen how regions with higher values of sky variance (higher variance in the sky brightness), are located in the borders of the images, where less detectors overlap, i.e., regions with less exposure time. Also, at the borders of the detectors, where they overlap one with another, there is less sky variance.

The origin of the overdensity region seen in Figure 4.1a is also clear. In this region, a higher overlap of detectors is appreciable, what implies less sky variance and, therefore, more detected objects. This same region also has higher S/N values, as can be seen in Figure 4.2a, where warmer colours means a higher S/N with respect to the other

regions. This can be explained, again, by the larger number of overlapping detectors in this region, that lead to a higher S/N. In this same figure, it can be seen how the borders of the images considered present less S/N than other regions, as these borders got less sampled (less detector overlap).

In any case, and apart from these patterns that are formed during the process of image coaddition, the values of S/N and sky variance are normal, and we do not see any unexpected malfunctioning of the taking/reduction of images.

Also, the distribution of ellipticities is shown in Figure 4.2c (stars) and Figure 4.2d (galaxies). First, it should be noted how the regions with higher object density are correctly represented again on these plots. In general, it can be seen how the detection of stars was correctly made, as the objects catalogued as such have a constant distribution of ellipticity, smaller than that of objects considered galaxies. The values for the ellipticity of stars are very close to zero, what, as was said, assure a good image quality.

In Figure 4.2d, we see that the ellipticity values for galaxies are higher, as expected. It can also be seen an increase of the ellipticity on the stripes formed by the images border, regions that, as can be seen in Figure 4.2a, got less coadded images. As in these regions the noise is higher, the distortion of the object could be more marked, meaning a higher ellipticity in those regions.

Then, it can be confirmed a correct reduction and source extraction by the survey. Despite the variations found in the footprint, the values measured for the different parameters represented are as expected.

4.3 Image depth

It was also decided to evaluate the depth of the images considered. We will give the depth for $S/N = 5$. To do so, objects with a S/N close to 5 were selected, that means, objects detected with a signal five times greater than its noise. S/N can be expressed as (4.3).

While selecting EROs in the next chapter, only objects with $S/N > 5$ were considered. So, by showing the distribution of magnitudes with errors leading to a $S/N \simeq 5$, is possible to verify the depth of the sample, that is, in essence, the magnitude to which we are complete for sources with $S/N > 5$ (in SHARKS, this limit is theoretically set at $K_s = 22.7\ mag\ [AB, 5\sigma]$).

This is precisely what can be seen in Figure 4.3. The results obtained are shown as a scatter plot with the variation in magnitude of the objects considered (those with $S/N \simeq 5$) (see Figure 4.3a), and a histogram that shows the distribution of magnitudes (see Figure 4.3b). The detector overlap, commented in the previous sections, are clearly visible in Figure 4.3a. These overlaps lead to a higher image depth.

The mean and standard deviation values of this distribution is shown in Equation

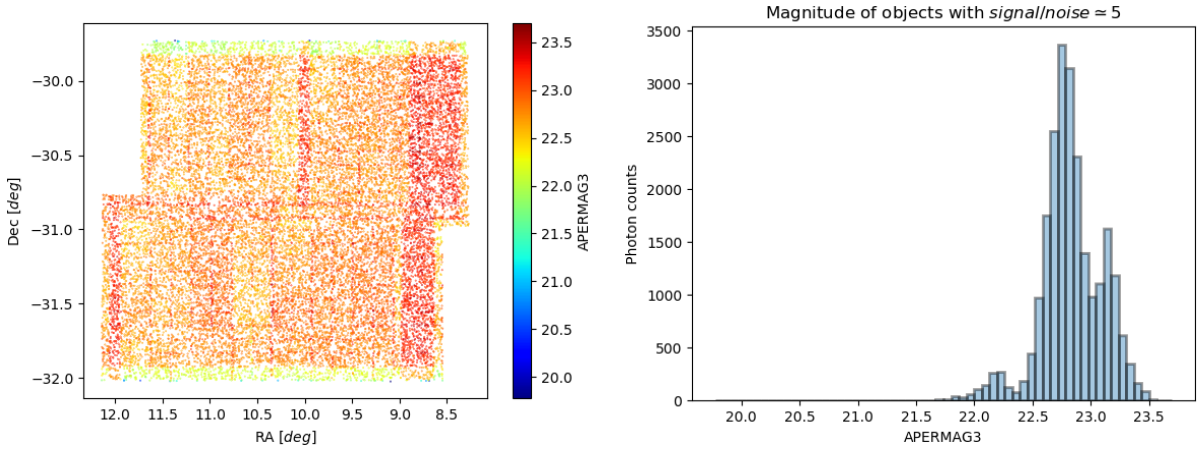

(a) *Angular distribution of magnitude values for sources with* $S/N \simeq 5$.

(b) *Magnitude distribution for sources with* $S/N \simeq 5$.

Figure 4.3: *Magnitude distribution for objects with* $S/N \simeq 5$. *In* ***(a)*** *this magnitude is represented over the footprint (with both axis in degrees), and in* ***(b)*** *as an histogram. The magnitudes represented are, in both cases "APERMAG3", aperture magnitudes measured within 2 arcseconds. The median magnitude of the distribution is of the order of the theoretical value (*$22.7\ mag\ [AB, 5\sigma]$*)*

.

4.4, which we quote as the experimental image depth.

$$Image\ depth\ (experimental) : K_s = 22.82 \pm 0.28\ mag\ [AB, 5\sigma] \tag{4.4}$$

In average, we obtain a depth that is higher than the expected value ($22.7\ mag, AB, 5\sigma$), so this means that the measured depth is even better than planned. This way, it can be confirmed the potential that SHARKS has, verifying the magnitude limit, and for a wide area.

4.4 Astrometry

One of the most important aspects to verify in any astronomical catalogue is the reliability of its astrometry *(Seidelmann et al. 2002)*.

SHARKS DR1 has been astrometrically calibrated with respect to the 2MASS point source catalogue *(Cutri et al. 2003)*. To verify it has been correctly calibrated, we compare the angular distance and differences in right ascension and declination between SHARKS sources and the two catalogues considered to check astrometry.

The cross-matching is a technique applied in astronomy to associate objects in differ-

ent catalogues, in order to combine information from different observations into the same matched objects. The match between catalogues was made by the use of the `Python` module `Smatch` (Appendix A.8). In what follows, we use 1 arcsecond matching radius between the catalogues.

As it was explained in Chapter 3, the catalogues considered to verify SHARKS DR1 astrometry are 2MASS and *Gaia* (sections 3.1 and 3.2). The SHARKS-2MASS matching lead to a catalogue of 9124 objects present in both catalogues, and the SHARKS-*Gaia* to a sample of 18286 sources present in both SHARKS and *Gaia*.

The formula used to obtain the angular distance between the matched sources is (eq. 4.5):[9]

$$\begin{aligned}\cos\gamma = \cos(90^\circ - \mathrm{Dec}_1)\cos(90^\circ - \mathrm{Dec}_2) + \\ + \sin(90^\circ - \mathrm{Dec}_1)\sin(90^\circ - \mathrm{Dec}_2)\cos(\mathrm{RA}_1 - \mathrm{RA}_2) \leftrightarrow \\ \leftrightarrow \gamma = \arccos[(90^\circ - \mathrm{Dec}_1)\cos(90^\circ - \mathrm{Dec}_2) + \\ + \sin(90^\circ - \mathrm{Dec}_1)\sin(90^\circ - \mathrm{Dec}_2)\cos(\mathrm{RA}_1 - \mathrm{RA}_2)] \quad (4.5)\end{aligned}$$

Where Dec_1 and RA_1 are the declination and right ascension of each object in the first survey considered, Dec_2 and RA_2 the same quantities but in the other survey, and γ the angular distance between the position of the objects in the two matched catalogues considered.

Next, we present the differences in right ascension (RA) and declination (Dec), as well as the angular distance (γ, calculated with equation 4.5), between matched sources in SHARKS-2MASS (see Figure 4.4a) and in SHARKS-*Gaia* (see Figure 4.4b).

The angular distances for both calibration catalogues can be more clearly seen in Figure 4.5, where we show the angular distances (γ) between objects detected in SHARKS-2MASS and SHARKS-*Gaia*.

It was also calculated the medium value of γ, δ_{RA} and δ_{Dec} for each comparison of catalogues, and the standard deviation respect to the medium, indicated as the error (Equations 4.6, 4.7).

$$\begin{aligned}\gamma_{(SHARKS-2MASS)} &= 0.333 \pm 0.219\ [arcseconds] \\ \delta_{RA(SHARKS-2MASS)} &= -0.001 \pm 0.358\ [arcseconds] \\ \delta_{Dec(SHARKS-2MASS)} &= -0.007 \pm 0.271\ [arcseconds] \quad (4.6)\end{aligned}$$

[9] M. Richmond. Precession, Proper Motion, and Angular Separation. `http://spiff.rit.edu/classes/phys301/lectures/precession/precession.html`

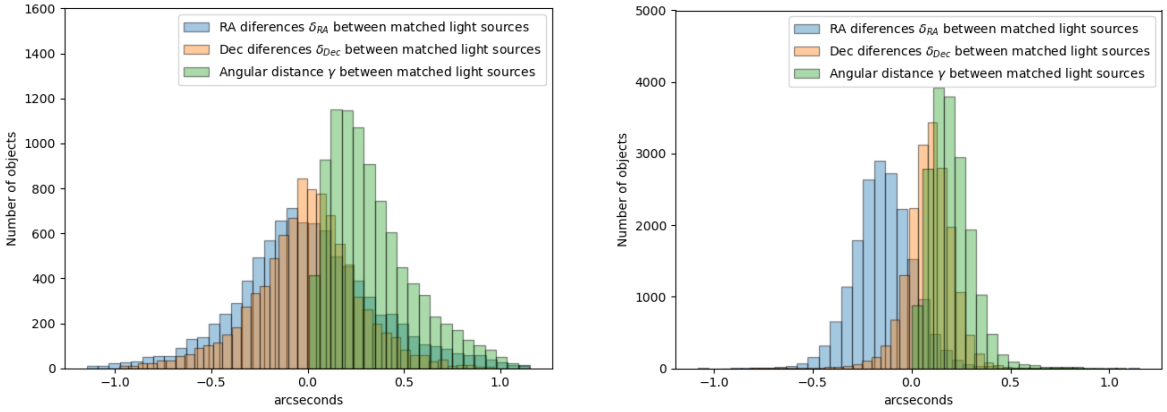

(a) *Astrometrical comparison in SHARKS-2MASS.*

(b) *Astrometrical comparison in SHARKS-Gaia.*

Figure 4.4: *Histograms showing the difference between RA (δ_{RA}), Dec (δ_{Dec}) and the angular distance (γ) between positions in both catalogues (SHARKS-2MASS **(a)** and SHARKS-Gaia **(b)**), measured in arcseconds.*

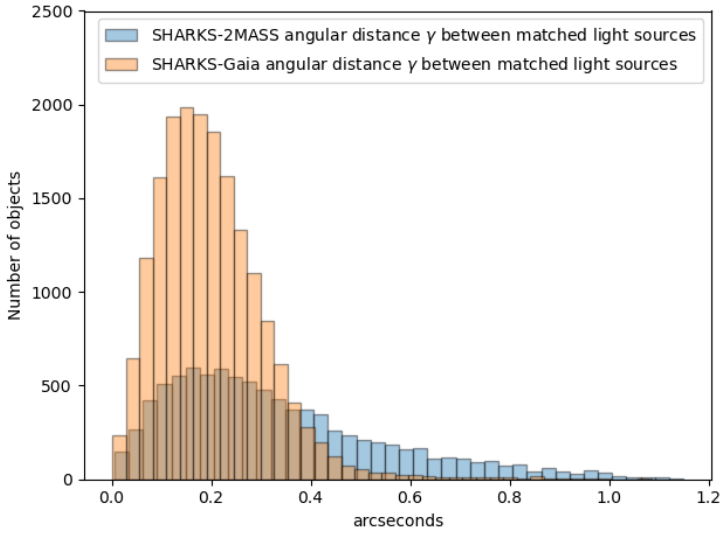

Figure 4.5: *Angular distance γ between the position of matched objects on SHARKS-2MASS and SHARKS-Gaia. The distances are measured in arcseconds.*

$$\begin{aligned} \gamma_{(SHARKS-Gaia)} &= 0.200 \pm 0.110 \ [arcseconds] \\ \delta_{RA(SHARKS-Gaia)} &= -0.141 \pm 0.159 \ [arcseconds] \\ \delta_{Dec(SHARKS-Gaia)} &= -0.092 \pm 0.123 \ [arcseconds] \end{aligned} \tag{4.7}$$

To check the astrometry, the focus should be put in the δ_{RA} and δ_{Dec} values. In the SHARKS-2MASS comparison, the medium difference between RA and Dec measures is in both cases very close to zero, the expected result, as SHARKS is astrometrically calibrated respect 2MASS. These differences are notoriously bigger for SHARKS-*Gaia*.

It can be seen a higher dispersion of γ values for SHARKS-2MASS than for SHARKS-*Gaia*. This result can be understood taking into account that 2MASS observed from the Earth, while *Gaia* from space, so distortions from the atmosphere are not present in *Gaia* measures.

The distances γ shown in both equations (4.6 and 4.7) are smaller than the pixel size of SHARKS images (0.34 arcseconds), what reflects a good correlation between the positions of objects measured by SHARKS, and those measured by the surveys dedicated to map the sky, 2MASS and *Gaia*. With this, it can be considered validated the astrometry of the SHARKS DR1 catalogue.

4.5 Photometry

To end the verification of SHARKS DR1, we look at the photometry. As it was commented in Chapter 3 (section 3.3), the catalogue used is the second Data Release of VIKING.

The verification consists in the comparison of magnitudes measured in both catalogues (SHARKS and VIKING). The matched SHARKS-VIKING catalogue have 239898 objects. To check the photometry, the SHARKS-VIKING catalogue was first cleaned from objects with signal to noise ratio (eq. 4.3) smaller than 5. Also, only stars were considered by the use of the "classstat"[10] parameter, provided by `SExtractor`[11] (considering objects with: $classstat > 0.9$). This parameter will be explained in more detail below. The final SHARKS-VIKING matched catalogue passed after applying these criteria to have 71801 objects.

SHARKS magnitudes are calibrated with respect to AB, while VIKING with Vega; so, by the analysis of the differences between the magnitudes measured in both catalogues, is possible to verify the correctness of SHARKS calibration. To do this, it is necessary to know the difference between Vega and AB calibrated magnitudes, difference shown in the equation 4.8. Is important to notice that this conversion is for K_s magnitudes.[12]

$$K_{s,AB(SHARKS)} - K_{s,Vega(VIKING)} = 1.827 \tag{4.8}$$

[10] Classstat (also called CLASS_STAR) documentation. `https://sextractor.readthedocs.io/en/latest/ClassStar.html`

[11] SExtractor (Source-Extractor), the program used to reduce SHARKS images. `https://sextractor.readthedocs.io/en/latest/Introduction.html`

[12] Cambridge Astronomy Survey Unit (CASU). VISTA Filter Set. `http://casu.ast.cam.ac.uk/surveys-projects/vista/technical/filter-set`

This is the expected calibration difference. In order to obtain the experimental one, a polynomial fit of order zero was made (assuming linearity), comparing the values of magnitudes that each object matched have in SHARKS and in VIKING. This fit gives a value of the origin ordinate, that indicates the calibration difference between SHARKS and VIKING. The result is shown in Figure 4.6, where magnitudes are both aperture magnitudes of 2 arcseconds.

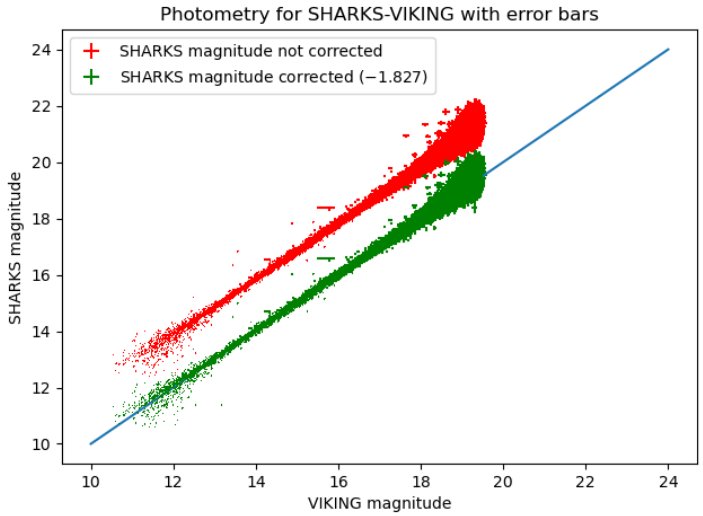

Figure 4.6: *Comparison of magnitudes between SHARKS and VIKING. Red dots indicate the original data without corrections, and green dots those obtained after applying the experimental transformation calculated (-1.827) to change AB magnitudes (SHARKS originals) to Vega magnitudes (VIKING). The error bars show the errors in the magnitude measures for each survey. The line shows the ideal behaviour after the application of the correction.*

The experimental difference obtained is (4.9):

$$K_{s,AB(SHARKS,exp)} - K_{s,Vega(VIKING,exp)} = 1.827 \tag{4.9}$$

The theoretical and experimental values of the difference between K_s magnitudes calibrated in AB (SHARKS) and in Vega (VIKING) are exactly the same, what indicates that the calibration of SHARKS is correctly set. It also confirms the equivalence between magnitudes measured by SHARKS and those obtained by VIKING.

Considering both aspects previously commented, it can be ensured the correctness of the SHARKS DR1 photometry, that means, the correct magnitude measurement by the survey.

With this, all the different procedures considered in the first SHARKS catalogue

validation concluded. The results obtained were the expected ones, and in any of the processes developed we saw any pathological issue, so, finally, it can be confirmed the reliability of SHARKS DR1.

In addition to this, it is important to mention that, even if the final Data Release 1 will be compounded by 13 deg^2 of more data, the verifications applied to the sample considered could be used as an evidence of the correctness of all the 20 deg^2 that will take part of the final DR1 catalogue. In any case, if it is wanted to prove the same tests in the total amount of data, the employed `Python` programs, shared in `GitHub` (Annexe A.1), could be used with the total DR1 catalogue.

Chapter 5

Design and study of an EROs catalogue from SHARKS DR1

Tras validar el SHARKS DR1, es posible ya emplear sus datos para la investigación científica que se ha considerado: el diseño de un algoritmo para buscar los objetos extremadamente rojos (EROs) presentes en el DR1. Se comenta en este capítulo el proceso llevado a cabo hasta la obtención de la muestra final de EROs, desde el filtrado del DR1 para eliminar la mayor cantidad de objetos espurios presentes en él, pasando por el diseño de un algoritmo para diferenciar correctamente estrellas y galaxias con el fin de eliminar la contaminación por enanas marrones en la muestra de EROs, y mostrando finalmente el resultado que se obtiene, con una serie de cut-outs de los EROs encontrados.

After the validation of the SHARKS DR1 catalogue, the ambitious possibilities that SHARKS offers to study the sky at NIR wavelengths are explored. In particular, we create a catalogue of EROs, objects very faint in the optical but bright in the NIR. To do so, optical data from DES will be used in combination with SHARKS K_s band.

5.1 Cleaning the SHARKS DR1 catalogue

SHARKS DR1 catalogue has 623543 objects. From this sample, only those objects with a signal to noise ratio (eq. 4.3) greater than 5 were considered. Also, we removed detections made near diffracted stars, in order to eliminate as many spurious objects as possible.

After applying these corrections, by the use of `Topcat`, the original catalogue passed from having 623543 objects to have 482942. In Figure 5.1 two examples of the cleaning process are shown.

After cleaning the sample from possible spurious sources, it is ready to be used, in

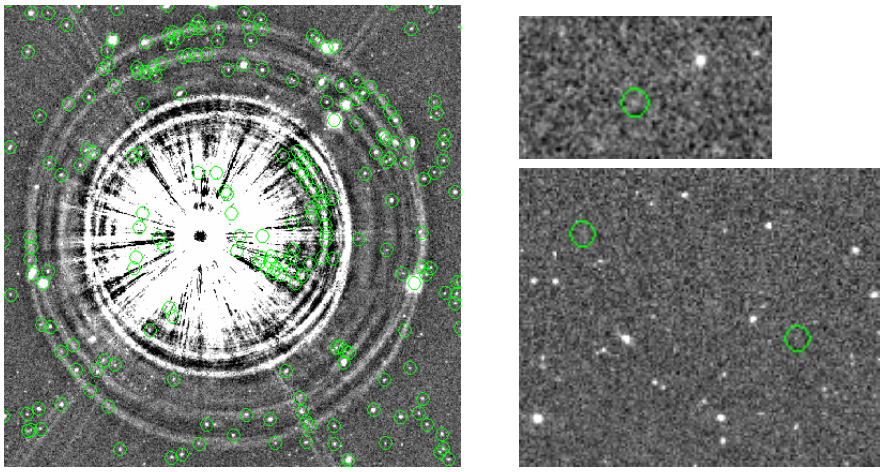

(a) *A diffracted star, leading to a high level of spurious objects.*

(b) *Ambiguous detections (low S/N).*

Figure 5.1: *Examples of spurious objects that were removed from the SHARKS DR1 catalogue, caused by diffracted stars* ***(a)*** *and detections with low S/N* ***(b)****.*

our case, to search for EROs. But, to do so, first we need to define stars and galaxies in our catalogue, therefore the development of a correct algorithm of classification was needed.

5.2 The star/galaxy classification

The method used to classify objects as stars and galaxies was developed by replicating the method used in *Daddi et al. 2000*. In this article, objects with magnitudes $R\ [Vega, 5\sigma]$ and $K_s\ [Vega, 5\sigma]$ over certain values are all considered galaxies, while for brighter magnitudes, the morphological parameter, "classstat"[10] is used.

"classstat" classifies objects between stars and galaxies, giving stars values closer to 1, and galaxies closer to 0. The bad functioning of this parameter at faint magnitudes can be understood taking in account that, at faint magnitudes, the angular size of the object is at the level of the seeing, so there are difficulties to correctly resolve if the object detected is a star or a galaxy.

SHARKS observes in the K_s band, therefore the limits used in *Daddi et al. 2000* were changed in our case, to consider a magnitude limit in the SHARKS band. To find the correct star/galaxy classification using the K_s band, a comparison of the number counts of stars and galaxies was done between our data and that from *Daddi et al. 2000*.

After a process of fine-tuning, Figure 5.2 was obtained. Here we show the number of stars and galaxies as a function of K_s, both for *Daddi et al. 2000* and this work.

After the definition of our star/galaxy classification, a good agreement between both surveys is found. In Figure 5.2 we show the quantities obtained in the article *Daddi et al. 2000* (with detections in 701 $arcmin^2$ at $K_s \leq 18.8$ mag [Vega, 5σ] and 447.5 $arcmin^2$ at $18.8 < K_s \leq 19.2$ mag [Vega, 5σ]), while for SHARKS they are found after the application of the classification (that will be explained next).

The K_s binning is the same as employed on *Daddi et al. 2000* (after applying transformation from Vega magnitudes to AB, the calibration used by SHARKS, Eq. 4.8), and include all the objects that have a magnitude in a certain range. It is important to remark that all the magnitudes used in this chapter are again magnitudes for an aperture of 2 arcseconds. In *Daddi et al. 2000*, it was used a combination of isophotal magnitudes for bright magnitudes and 2 arcseconds aperture magnitude for faint ones. The magnitude limit for the *Daddi et al. 2000* sample is: $K_{s,Vega} = 19.2 \leftrightarrow K_{s,AB} = 19.2 + 1.83 = 21.03 \rightarrow K_s = 21.03\ mag\ [AB, 5\sigma]$.

The face values presented in Figure 5.2 are given in the Appendix, in Table B.1. Here we see the division of the 482942 objects that conform the original sample, between stars and galaxies. Likewise, from Figure 5.2 we see how the amount of galaxies starts to dominate over stars at $K_s \approx 19.2$. The saturation in the detection of stars is a expected result, since the observation of stars is only available for objects within our galaxy, so it is normal to not detect further stars once we reach a given faint magnitude limit. Also, SHARKS observations are done perpendicularly to the galactic plane, where less stars are found.

Finally, the star/galaxy separation algorithm defined for SHARKS (see Figure 5.2 and Table B.1) is:

- Objects with $K_s < 19.2$:
  Galaxies = Objects with $classstat < 0.5$
  Stars = Objects with $classstat \geq 0.5$

- Objects with $K_s \geq 19.2$:
  Galaxies = Objects with $classstat < 0.975$
  Stars = Objects with $classstat \geq 0.975$

This algorithm has almost the same performance as the algorithm defined in *Daddi et al. 2000*, but it does not imply the use of the R band and goes to fainter magnitudes.

In our method, K_s magnitudes are given on the AB system and $classstat$ is a probabilistic parameter provided by `SExtractor`[11] to separate between stars and galaxies (a value closer to 0 means galaxies, and closer to 1 means stars) that, as was said, does not work very well when we go to faint magnitudes.

With this new algorithm to classify objects in SHARKS between stars and galaxies, the cleaning of UCDs from the EROs catalogue is now possible.

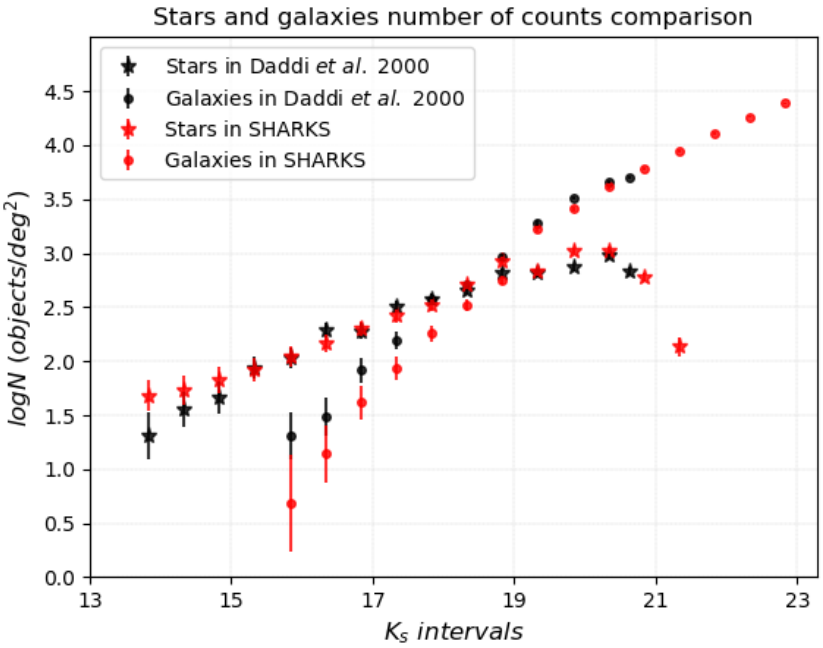

Figure 5.2: *Comparison between the abundance of stars and galaxies measured by SHARKS and those measured in Daddi et al. 2000. The K_s bins are those considered in Daddi et al. 2000, after applying the transformation from Vega magnitudes to AB. Error bars are only poissonian.*

5.3 The EROs-finder algorithm

The process followed to select EROs from the SHARKS DR1 catalogue is now explained.

As was commented in Chapter 2, we first need to associate SHARKS sources with those coming from an optical survey. In this case, the DES second Data Release catalogue (DES-DR2) was the chosen one. The original equation used to select EROs is (5.1):[3]

$$R_{Vega} - K_{s,Vega} > 5.5 \tag{5.1}$$

But the magnitudes r and K_s used respectively by DES and SHARKS are different from those employed in equation 5.1, so a translation to $r_{DES,AB}$ and $K_{s,AB}$ was needed. In this case, we use eq. 4.8 to transform K_s (taking $1.827 \simeq 1.83$), and eq. 3.1 to transform the R-band.

Finally, the colour parameter used to select EROs with DES-DR2 r and SHARKS-DR1 K_s bands is Equation 5.2.

$$R_{Vega} - K_{s,Vega} > 5.5 \leftrightarrow (r_{DES,AB} - 0.65) - (K_{s,AB} - 1.83) > 5.5 \leftrightarrow$$
$$\leftrightarrow r_{DES,AB} - K_{s,AB} + 1.18 > 5.5 \leftrightarrow \boxed{r_{DES,AB} - K_{s,AB} > 4.32} \quad (5.2)$$

Where $r_{DES,AB}$ are the magnitudes of the matched objects measured by DES in the r band, and $K_{s,AB}$ those of the same objects measured by SHARKS in the K_s band. To get information of the $r_{DES,AB}$ band for objects present in SHARKS DR1 catalogue, we made a 1 arcsecond spatial matching between both.

Before applying the selection, we investigate the properties of the matched sample. First we represented the different values of $r_{DES,AB} - K_{s,AB}$ (henceforth $r_{DES} - K_s$). In these plots, also the star/galaxy classifier developed was used, to study the colours that stars and galaxies have. The colour selection used to consider objects as EROs is also represented (see Figure 5.3).

In these images, only objects with DES detections in the r_{DES} band were considered. Matched objects (with detection in the redder bands of DES) but undetected in the r_{DES} band were also considered in our EROs sample, but not in these figures. Also, in our EROs sample we keep objects that are directly not present in DES-DR2 as well.

For galaxies in SHARKS-DES, we also calculated $r_{DES} - K_s$ colours (see Figure 5.4) and median colours (see Table B.2) as a function of K_s magnitude.

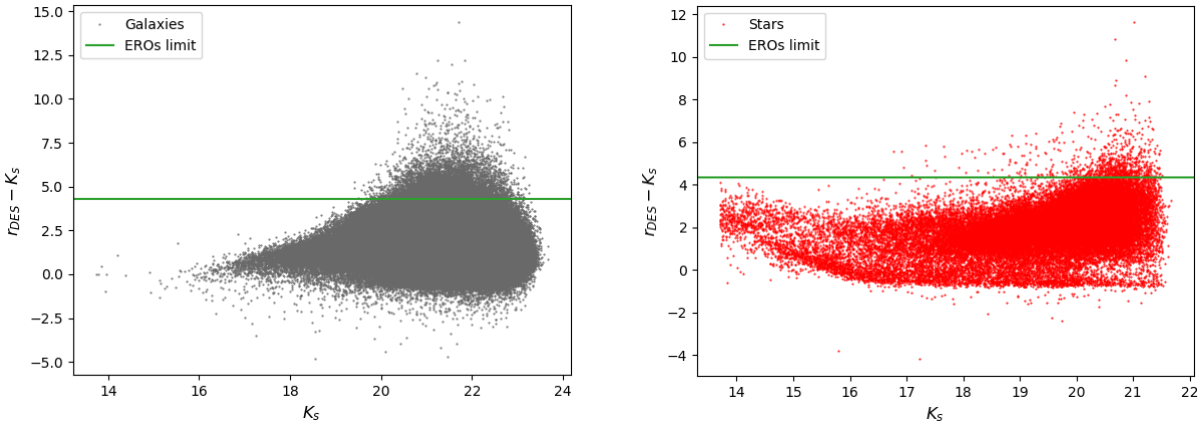

(a) *Galaxy colours* **(b)** *Star colours*

Figure 5.3: *$r_{DES} - K_s$ as a function of K_s for objects with detections in r_{DES}; for galaxies **(a)** and stars **(b)** matched between SHARKS DR1 and DES DR2 catalogues. The limit used to select EROs is indicated with a green line. Ojects above it are considered EROs.*

Figure 5.3 shows that a substantial part of the objects overpasses the EROs limit. In Figure 5.4, it can be seen the variation in the quantity of galaxies and the colours

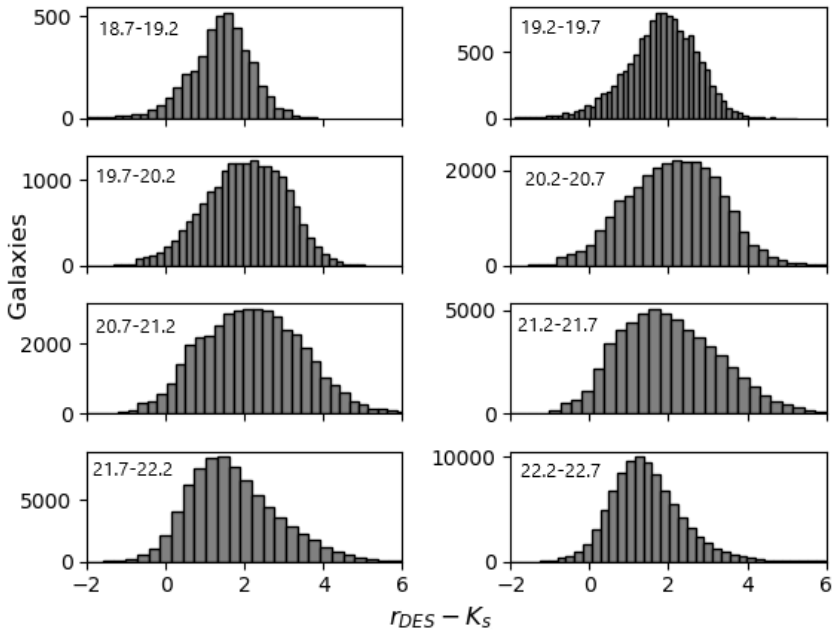

Figure 5.4: *Histograms of $r_{DES} - K_s$ for different magnitude intervals, only for galaxies matched between SHARKS DR1 and DES DR2 catalogues. The magnitude ranges are indicated on the top left corner in each histogram.*

of them as the K_s magnitude is increased. This same behaviour is shown in Table B.2, where the tendency to redder objects at fainter magnitudes is clearly appreciable.

Finally, objects present in both catalogues that verify eq. 5.2 were directly considered EROs. But, because of the potential that SHARKS has to observe in the NIR, we go one step further and add to the mentioned list, all the objects detected by SHARKS but not by DES.

Finally, the total EROs-finder algorithm consists of:

- Objects detected by SHARKS and DES (matched) that verify (5.2).
- Objects detected by SHARKS, but not by DES.

In the next section, this algorithm will be applied to the DR1 catalogue, already cleaned from objects with $S/N < 5$ and from objects around diffracted stars.

5.4 The EROs sample

After the application of EROs finder, we find 69625 objects classified as EROs, from the 482942 objects present in the parent catalogue. 11291 of them are detected by SHARKS

and DES, passing the colour cut defined in Equation 5.2, and 58334 are objects detected by SHARKS, but not present in DES. A certain amount of contamination by spurious sources is expected in this last group of objects, as no comparison with other surveys was made.

Next, we clean the sample of stars, which at these colour ranges, are mostly UCDs. Therefore, the algorithm to select stars and galaxies previously explained was applied on the EROs sample. This way, we remove all the stars that were classified as EROs. This sample is interesting in itself for UCDs searches, but it is out of the scope of this work. In Table 5.1 we show the final numbers of EROs and UCDs found in the SHARKS-DR1 sample.

Objects detected as EROs = 69625	
Galaxies = 68073	Stars = 1552

Table 5.1: *Result of applying the star/galaxy classification to the EROs sample. 98% are extragalactic and the rest UCDs.*

Henceforth, we will consider as EROs only these 68073 galaxies. The spatial distribution of these EROs can be seen in Figure 5.5.

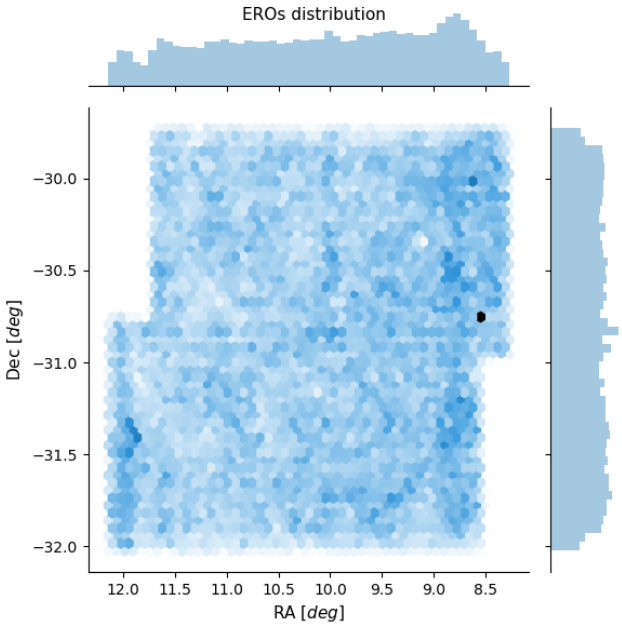

Figure 5.5: *Spatial distribution of the EROs sample, compounded by objects detected by SHARKS and not by DES, and objects detected by both catalogues that verify equation 5.2. This is the sample cleaned from UCDs.*

In Figure 5.5, some overdensities are detected. We have done a visual inspection of

the sample with `DS9`, in order to confirm if these overdensities are true EROs cluster candidates. In Figure 5.6 we show two of these clusters candidates:

- In the first case (Figure 5.6a), it is clear that many of the detections are actually starburst regions in the arms of the galaxy, therefore belonging to the same system and discrediting it as a cluster. This image shows that our EROs-detection algorithm does not work properly in the case of star-forming regions in nearby galaxies, where the algorithm associates these regions with EROs. This galaxy corresponds with the darker spot that can be observed in Figure 5.5.
- In the second case (Figure 5.6b), it is not so clear and it could possibly be a true overdensity of EROs, although it could also be associated with the extended galaxy. The search for EROs cluster candidates stopped here, although it will be continued by the SHARKS Collaboration in the future.

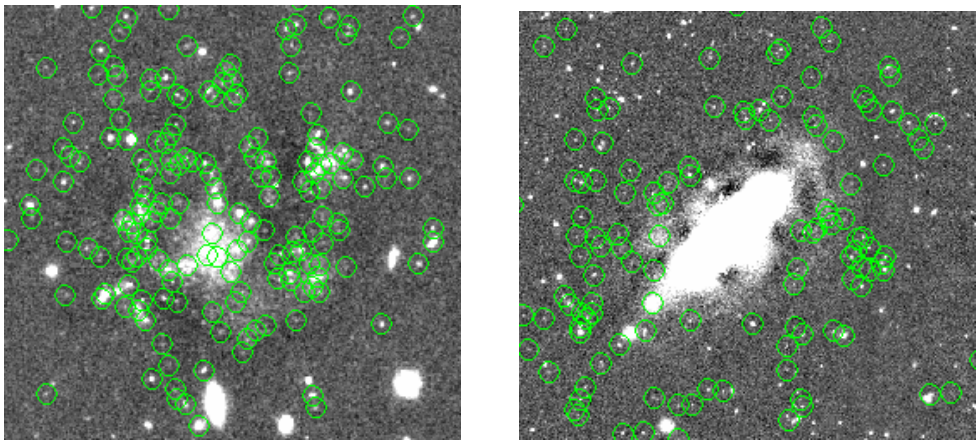

(a) **(b)**

Figure 5.6: *EROs overdensities, examined at DS9.* ***(a)*** *Dusty starbust that lead to a lot of miss-detections of EROs (in particular, this starbust is ESO 410-18).* ***(b)*** *An elliptical with lots of EROs detections, some of them associated to the galaxy, and other ones apparently not (this galaxy is NGC 254).*

When doing the visual inspection, we still found spurious objects around diffracted stars or with low detection level. Nonetheless, we consider the EROs sample has a high completeness and purity level, but with a certain degree of contamination. In any case, possible contaminants are a small part of the sample. To obtain a purer (but probably less complete) sample, a S/N of 10 could have been applied.

Finally, in Figure 5.5 we see a higher detection rate on the right of the image, where there is more exposure time. To confirm if this is true, we measured the density of EROs as a function of exposure time. In Figure 5.7 it can be seen how the density of

EROs detected increase at higher exposure times. This is a normal behaviour, taking in account that EROs are, in general, faint objects, so a longer exposure time will increase the detection sensibility.

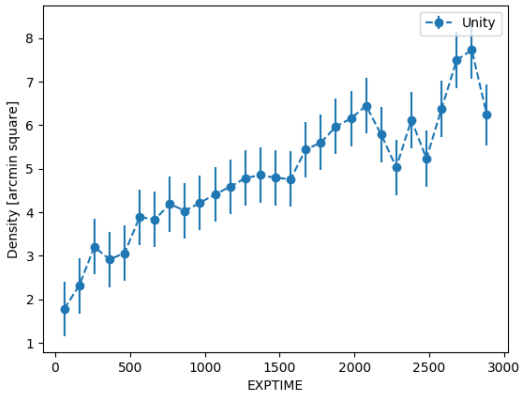

Figure 5.7: *Variation of the EROs number density as a function of exposure time (in seconds). As expected, in regions with higher exposure time we detect more EROs.*

We further analysed the amount of EROs as a function of magnitude. In Table 5.2 we show the cumulative number of EROs for different K_s magnitude limits. It can be seen how the number of EROs detected increase significantly from $K_s \approx 19.2$ and how the fraction with respect to the total number of galaxies increases as well. This is the expected behaviour, as we go to fainter magnitudes, the median galaxy colours (see Table B.2) gets redder and therefore, the fraction of EROs increases.

In Table 5.2 we also show the fraction of EROs with respect to the total galaxy density, calculated as the number of EROs divided by the 7.23 deg^2 sampled in the SHARKS DR1 catalogue (in arcminutes).

These quantities were compared with those obtained by the EROs sample from *Daddi et al. 2000*. In *Daddi et al. 2000* the limiting magnitude is $K_s = 21.03\ mag\ [AB, 5\sigma]$, so only quantities until these magnitudes were compared. We found a very good agreement between our results and those from *Daddi et al. 2000*, both in density and in the fraction of EROs with respect to all galaxies.

With these values, we can forecast the total number of EROs in SHARKS for the 300 deg^2. This estimate is shown in Table 5.3. To obtain this number, we used the density of EROs for magnitudes under SHARKS nominal depth ($K_s \leq 22.7\ mag\ [AB, 5\sigma]$). More than 2.2 million EROs are expected in the SHARKS footprint. Some spurious objects are expected even after the different cleanings applied to the catalogue, so the real EROs sample will be smaller.

Magnitude $[AB, 5\sigma]$	Number of EROs	Frac. $[EROs/\ Galaxies]$	Dens. $[arcmin^{-2}]$
$K_s \leq 19.2$	108	0.012	0.004
$K_s \leq 19.7$	256	0.012	0.010
$K_s \leq 20.2$	660	0.017	0.025
$K_s \leq 20.7$	2194	0.032	0.084
$K_s \leq 21.2$	6010	0.053	0.231
$K_s \leq 21.7$	14218	0.081	0.546
$K_s \leq 22.2$	30100	0.113	1.156
$K_s \leq 22.7$	54527	0.143	2.095
$K_s > 22.7$	68073	0.155	2.615

Table 5.2: *Cumulative numbers of EROs (after filtering the contamination of UCDs) at each K_s limiting magnitude. Frac. indicates the fraction of EROs respect to the total of galaxies measured in SHARKS DR1. Dens. indicates the number of EROs divided by the 7.23 deg^2 observed in SHARKS DR1 (in arcminutes).*

Magnitude limit $[AB, 5\sigma]$	EROs density $[arcmin^{-2}]$	Area $[deg^2]$	Number of EROs
$K_s \leq 22.7$	2.095	300	2262600

Table 5.3: *Estimation of EROs present in the 300 deg^2 that will make SHARKS data, using the density of EROs obtained in Table 5.2.*

5.5 EROs cut-outs

The brightness of the EROs population in the infrared is something easily appreciable by the comparison of observations of these objects in the NIR and in the optical. To make this comparison, we use the `Python` module `Astrocut` (Appendix A.10) to obtain cut-outs of some of the EROs detected in SHARKS at the NIR K_s band (2.2 microns), and in DES r and z bands.

A series of different cut-outs are now showed, to emphasize the robustness of the algorithm we developed. With this, the EROs finding was completed, obtaining a catalogue of EROs, correctly cleaned from UCDs and spurious sources. This preliminary analysis proves the utility of SHARKS to study these unique objects and the high-redshift Universe.

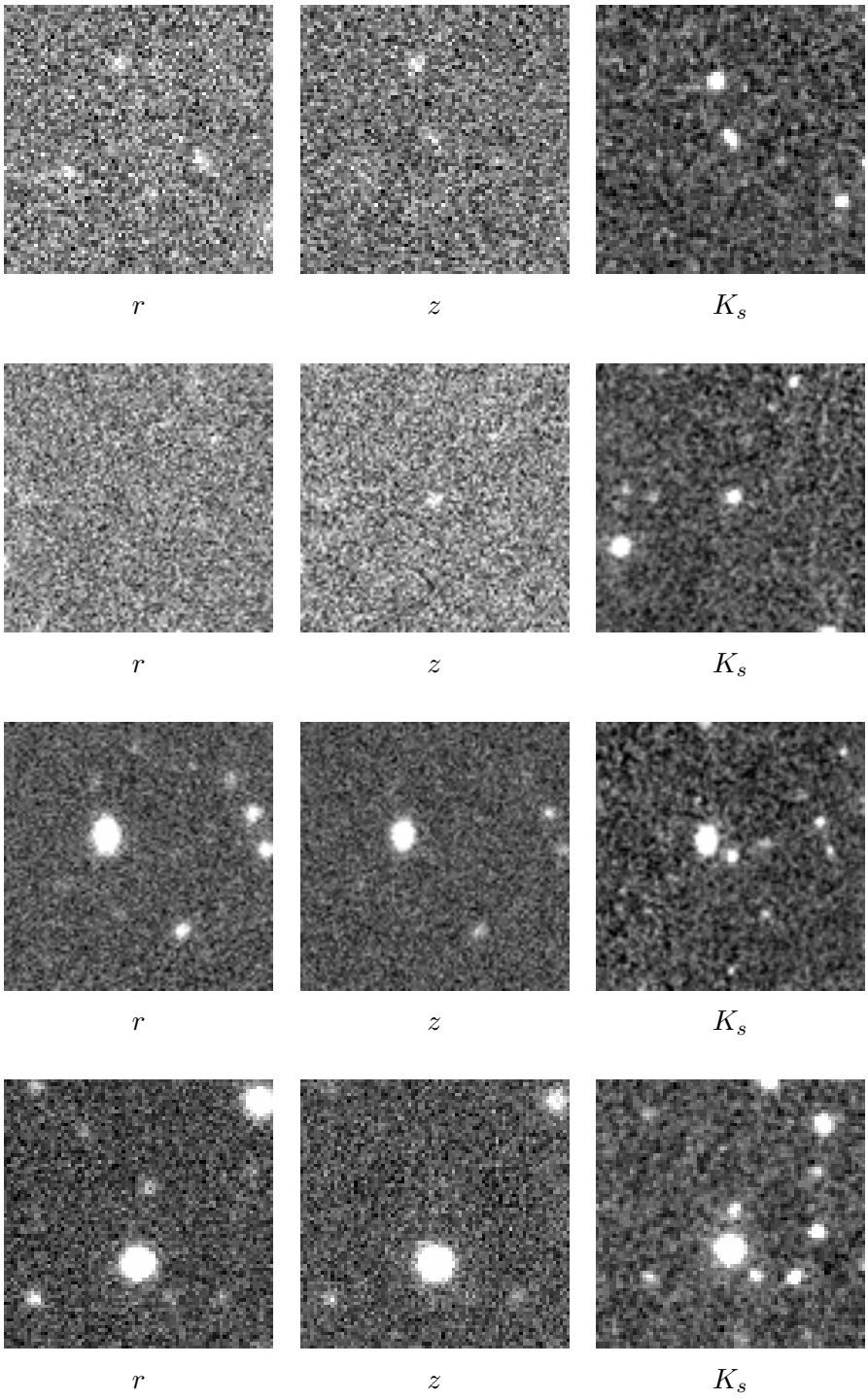

Figure 5.8: *EROs cut-outs. It can be seen the difference between observations in the r and z bands by DES, where EROs are faint or not visible, and these in the K_s band by SHARKS, where EROs look bright.*

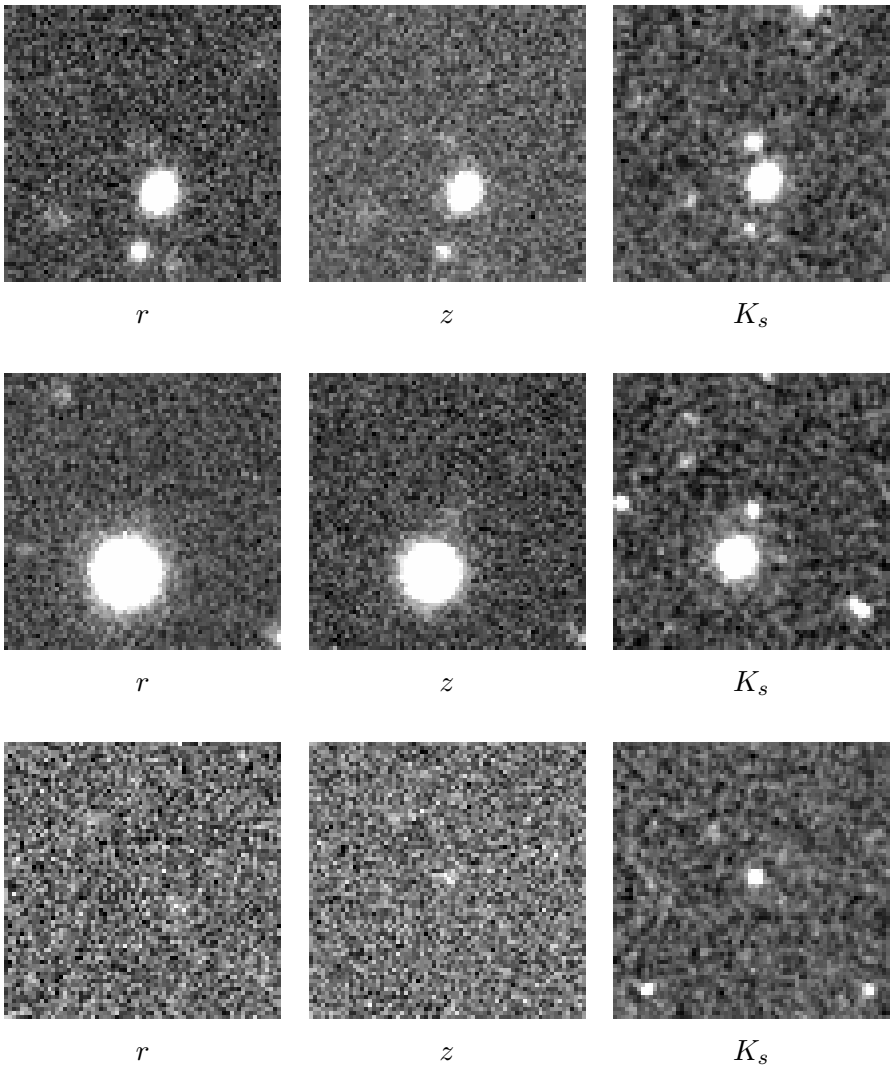

Figure 5.9: *Stars detected as EROs, probably UCDs. These stars are only visible in the K_s band images.*

Chapter 6

Conclusions

Para terminar, se listan en este capítulo los principales resultados obtenidos en el TFG, y se comentan las nuevas vías de estudio que pueden desarrollarse partiendo de las ideas planteadas en este trabajo.

Firstly, we made a complete verification of the DR1 catalogue, by the development of different `Python` codes, easily adaptable to other Data Releases of the project and to other surveys. From this data analysis, we summarize the following:

- The correct image reduction was verified looking at the distribution of several image properties.
- We found in average, a deeper magnitude limit than it was expected by design, what, definitely, are good news.
- In the astrometric comparison with 2MASS, δ_{RA} and δ_{Dec} values $\simeq 0$ were obtained, showing the good astrometric relation between both surveys.
- Also, a good result was obtained from the photometry check between SHARKS and VIKING, confirming that SHARKS calibration is correctly set.

The main results of the EROs study developed are:

- The EROs algorithm developed by the observations of SHARKS and DES lead to the detection of more than 68000 of these objects in the 7.23 deg^2 considered. This algorithm also includes the cleaning of UCDs from the EROs sample. This same procedure can be used in other K_s bands surveys similar to SHARKS, and obviously in future Data Releases of the project, as long as they overlap with DES or other optical surveys (like the Hyper-Suprime Camera in the GAMA fields).

- The EROs sample obtained lead to some interesting results, like the fraction that these extragalactic objects represent from the total galaxies detected by the survey, measured as 0.143 for magnitudes under SHARKS nominal depth ($K_s \leq 22.7\ mag\ [AB, 5\sigma]$); or the surface density of EROs, measured as 2.095 objects by arcminute for the same magnitude limit.

- An estimation of the total number of EROs detected in the final SHARKS catalogue was made. This estimation leads to a sample of more than 2.2 million EROs in the 300 deg^2 that will compound the entire SHARKS catalogue ($K_s \leq 22.7\ mag\ [AB, 5\sigma]$) . It is important to remark that, even having cleaned the DR1 catalogue from UCDs, low signal to noise objects, and around diffracted stars, a portion of spurious objects is expected to be detected, so the real EROs sample will be a smaller.

- In addition to this study of EROs, also the median $r - K_s$ colour of the galaxies present in the DR1 catalogue was obtained from the comparison between SHARKS and DES, showing an increase from magnitudes in range $K_s = 16.2 - 16.7$ to $K_s = 20.7 - 21.2$, where is reached the peak value: median $r - K_s = 2.195$. From this magnitude K_s bin ($K_s = 20.7 - 21.2$) to the image depth theoretical limit ($K_s = 22.7$), the median colour decreases.

More advanced investigations, that were out of this work scope, can be developed with the EROs sampled:

- In the EROs distribution represented (Figure 5.5) some regions with EROs overdensities were observed. An EROs cluster finding can be developed by the study of the redshifts that objects located in these regions have.

- Other possible use of the EROs-finder algorithm developed in this study is to search for UCDs and star-forming regions in nearby galaxies; since those have similar properties to EROs.

- EROs are mostly conformed by star-forming galaxies and ellipticals at high redshift. In the future, SHARKS collaboration will study the angular correlation function of them, in order to analyse the EROs clustering and to prove the presence of high-z ellipticals on this sample.

During this work, we have developed several programs and analysis pipelines. All these programs are publicly available through `GitHub` in: `https://github.com/SergioSE98/TFG_1`

Bibliography

- Abbott T.M.C., Aldering G., Annis J., et al. 2005. The Dark Energy Survey.

- Abbott T.M.C., Adamow M., Aguena M., et al. 2021. The Dark Energy Survey Data Release 2.

- Afonso J., Mobasher B., Chan B. et al. 2001. Discovery of an Extremely Red Galaxy at z=0.65 with Dusty Star Formation and Nuclear Activity. ApJ, 559L, 101A.

- Brown A.G.A., et al., *Gaia* Collaboration. 2018. Summary of the contents and survey properties. A&A, 616A, 1G.

- Cuby J.G., Saracco P., Moorwood A.F.M., et al. 1999. Discovery of a faint field methane brown dwarf from ESO NTT and VLT observations. A&A 349, L41.

- Cutri R., Skrutskie M., Dyk S., et al. 2003. 2MASS All-Sky Catalog of Point Sources. VizieR Online Data Catalog.

- Daddi E., Cimatti A., Pozzetti L., et al. 2000. Detection of strong clustering of extremely red objects: implications for the density of $z > 1$ ellipticals. A&A 361, 535–549.

- Eales S., Dunne L., Clements D., et al. 2010. The Herschel ATLAS. Publications of the Astronomical Society of the Pacific, 122, 499.

- Edge A., Sutherland W., Kuijken K., et al. 2013. The VISTA Kilo-degree Infrared Galaxy (VIKING) Survey: Bridging the Gap between Low and High Redshift. The Messenger, 154, 32-34.

- Edge A., Sutherland W., Viking Team. 2016. VizieR On-line Data Catalog: II/343. Originally published in: 2013Msngr, 154, 32E.

- González-Fernández C., Hodgkin S.T., Irwin M.J., et al. 2017. The VISTA ZYJHKs Photometric System: Calibration from 2MASS. Monthly Notices of the Royal Astronomical Society, 2246, 0C.

- Honscheid K. and DePoy D.L. (for the DES Collaboration). 2008. The Dark Energy Camera (DECam).

- Ochsenbein F., Bauer P. and Marcout J. 2000. The VizieR database of Astronomical Catalogues. A&AS, 143, 23O.

- Oteo I., on behalf of the SHARKS collaboration. 2016. SHARKS: Southern H-ATLAS Regions Ks-band Survey, Phase 1 proposal.

- Oteo I., on behalf of the SHARKS collaboration. 2017. SHARKS: Southern H-ATLAS Regions Ks-band Survey, ESO Survey Management Plan Form.

- Prusti T., et al., *Gaia* Collaboration. 2016. Description of the *Gaia* mission (spacecraft, instruments, survey and measurement principles, and operations). A&A, 595A, 1G.

- Seidelmann P.K. and Kovalevsky J. 2002. Application of the new concepts and definitions (ICRS, CIP and CEO) in fundamental astronomy. A&A 392, 341-351.

- Skrutskie M.F., Cutri R.M, Stiening R., et al. 2006. The Two Micron All Sky Survey (2MASS). AJ, 131, 1163.

- Sutherland W., Emerson J., Dalton G., et al. 2015. The Visible and Infrared Survey Telescope for Astronomy (VISTA): Design, Technical Overview and Performance. A&A, 575A, 25S.

- Thompson D., Beckwith S.V.W., Fockenbrock R., et al. 1999. The surface density of Extremely Red Objects. ApJ, 523, 100.

Appendix A. Software employed

In this appendix are shown the different software used during this project.

1. `GitHub`: Provider of Internet hosting for software development and version control using Git. The development of the programs employed in this work was shared by this tool. `https://github.com`

2. `Python`: The programming language used to develop all the programs of this work. `https://www.python.org`

3. `NumPy`: Library for `Python` that add support for arrays and a large collection of mathematical functions. `https://numpy.org`

4. `Matplotlib`: Plotting library for the `Python` programming language and its numerical mathematics extension `NumPy`, that provides an object-oriented API for embedding plots into applications. `https://matplotlib.org`

5. `Pandas`: Software library for `Python` that offers data structures and operations for manipulating numerical tables and time series. `https://pandas.pydata.org`

6. `Seaborn`: `Python` data visualization library based on `Matplotlib` that provides a high-level interface for drawing attractive and informative statistical graphics. `https://seaborn.pydata.org`

7. `Astropy`: Collection of software packages written in the `Python` programming language and designed for use in astronomy, providing a series of core functionalities in the astronomic study. `https://www.astropy.org`

8. `Smatch`: A `Python` code for matching points on the sphere using healpix. `https://github.com/esheldon/smatch`

9. `PyFITS`: `Python` library that provides access to FITS files. `https://pyfits.readthedocs.io/en/latest`

10. `Astrocut`: `Python` module that provides tools for making image cut-outs from sets of images with shared footprints. `https://astrocut.readthedocs.io`

11. `SAOImageDS9`: Image display and visualization tool for astronomical data. `https://ds9.si.edu`

12. `Topcat`: Interactive graphical viewer and editor for tabular data capable of handling large and sparse datasets with correlation functionality. `http://www.star.bris.ac.uk/~mbt/topcat`

13. `Overleaf`: Collaborative cloud-based LaTeX editor used for writing, editing and publishing scientific documents. `https://es.overleaf.com/learn`

14. `Spyder`: Open-source cross-platform integrated development environment (IDE) for scientific programming in the Python language. `https://www.spyder-ide.org/`

15. `Google Colaboratory`: Free Jupyter Notebook environment that requires no configuration and runs entirely in the cloud. `https://colab.research.google.com/notebooks/intro.ipynb?utm_source=scs-index`

Appendix B. Tables

K_s *mag* range $[AB, 5\sigma]$	Stars	Galaxies
< 13.7	362	34
13.7-14.2	346	11
14.2-14.7	385	2
14.7-15.2	487	8
15.2-15.7	597	11
15.7-16.2	784	35
16.2-16.7	990	100
16.7-17.2	1237	298
17.2-17.7	1716	622
17.7-18.2	2278	1311
18.2-18.7	3643	2379
18.7-19.2	6111	4081
19.2-19.7	4877	12005
19.7-20.2	7618	18695
20.2-20.7	7658	29501
20.7-21.2	4311	43483
21.2-21.7	983	63289
21.7-22.2	0	90661
22.2-22.7	0	115752
> 22.7	0	56281
Total	44383	438559
Total objects detected = 482942		

Table B.1: *Differentiation between stars and galaxies of the sample of 482942 objects present in SHARKS DR1, using the modification of the "classstat" parameter considered for SHARKS. The K_s magnitudes shown are AB calibrated. $K_s = 22.7$ is the theoretical image depth for SHARKS $[AB, 5\sigma]$. The first bin is not represented in Figure 5.2.*

K_s *mag* range $[AB, 5\sigma]$	Galaxies	Median $r_{DES} - K_s$
13.7-14.2	6	0.085
14.2-14.7	1	-0.071
14.7-15.2	5	-0.626
15.2-15.7	9	-0.030
15.7-16.2	34	-0.200
16.2-16.7	97	0.133
16.7-17.2	293	0.477
17.2-17.7	616	0.681
17.7-18.2	1301	0.961
18.2-18.7	2363	1.131
18.7-19.2	4041	1.383
19.2-19.7	11865	1.824
19.7-20.2	18417	2.005
20.2-20.7	28749	2.143
20.7-21.2	41723	2.195
21.2-21.7	57938	2.041
21.7-22.2	76799	1.738
22.2-22.7	92360	1.463
> 22.7	42608	1.333

Table B.2: *Median colours ($r_{DES} - K_s$) of the galaxies present in the SHARKS DR1 − DES DR2 matched catalogue, that have been detected in the r_{DES} band, for each of the K_s bins considered. It can be clearly seen how the redder colours tend to be associated with more distant galaxies, that means, fainter ones. $K_s = 22.7$ is the theoretical image depth for SHARKS $[AB, 5\sigma]$.*